THE JOURNAL OF PHYSICAL CHEMISTRY B

pubs.acs.org/JPCB Article

Augmented Scaled Particle Theory

C. Z. Qiao, S. L. Zhao,* H. L. Liu, and W. Dong*

Cite This: J. Phys. Chem. B 2020, 124, 1207−1217 Read Online

ACCESS | Metrics & More | Article Recommendations

ABSTRACT: The original motivation for scaled particle theory (SPT) is to derive a simple equation of state for a bulk hard sphere (HS) fluid. It is now widely recognized that SPT provides also the surface tension of a HS fluid near a spherical hard wall, including three contributions, i.e., the planar surface tension and two bending rigidities due to the surface curvatures (integrated mean and Gauss curvatures). This conforms to the basic assumption of morphological thermodynamics. The existence of non-Hadwiger terms, i.e., higher-order curvature terms, has been evidenced recently. Augmenting SPT by only one non-Hadwiger term, i.e., third-order curvature term, allows us to obtain two new analytical theories, which not only describe very accurately bulk thermodynamic properties but also improve systematically surface ones with respect to SPT.

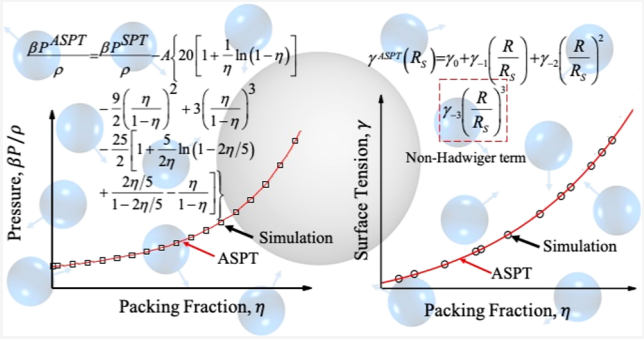

1. INTRODUCTION

Worked out by Reiss, Frisch, and Lebowitz in 1959,[1] scaled particle theory (SPT) has become a very successful theory in liquid physics with widespread applications.[2,3] Continuous efforts are made to extend and improve it (see, e.g., ref 4−28, which is by no means an exhaustive list of the very large number of papers on SPT in the literature). The initial motivation for SPT was to derive a simple equation of state for a bulk hard sphere (HS) fluid. It is now well recognized that SPT provides not only the bulk thermodynamic properties but also the surface tension of a HS fluid near a spherical hard wall. Within the framework of SPT, this surface tension includes three contributions, i.e., the planar surface tension and two bending rigidities due to surface curvatures, i.e., integrated mean and Gauss curvatures. Accompanying the investigation of more and more complex inhomogeneous systems, e.g., fluids adsorbed in nanoporous materials, there is an increasing need to understand better interfacial thermodynamic properties. Although early studies go back to Tolman,[29] it might appear surprising that our knowledge about curved interfaces is still quite limited. Mecke and co-workers have made efforts to develop a general framework, named morphological thermodynamics, to account for more complex surface morphology.[30−38] According to the Hadwiger theorem in integral geometry,[39,40] the morphological thermodynamics postulates that the thermodynamic potential of an inhomogeneous system is determined only by four terms, i.e., one bulk contribution proportional to the system's volume and three surface contributions proportional respectively to the surface area, mean, and Gauss curvatures of the interface. It is to be pointed out that in SPT, the work for forming a spherical cavity inside a HS fluid is assumed to have this form. The foundation of morphological thermodynamics has been questioned recently.[41−44] From molecular dynamics simulations, Laird et al. found that contributions from the higher-order curvatures to surface tension are not negligible.[41] Using the diagrammatic expansion of surface tension, Urrutia[43] and Hansen-Goos[44] showed, with exact analytic results, that the contribution of the third-order curvature term to the surface tension does not vanish. Now, it is clear that the contribution from the higher-order curvature terms is lacking in SPT. Is it possible to include some non-Hadwiger terms in SPT? Does this necessarily improve SPT? With a particular choice for the dividing surface to define the surface tension, this can be done straightforwardly, and some previous efforts have been devoted to this by Siderius and Corti.[16,17] In the present work, we explore another choice for the dividing surface and show the different strategies to circumvent the mathematical difficulty associated with our choice. It will be shown that including higher-order curvature terms does not guarantee an overall improvement of SPT. How can non-Hadwiger terms be included in a simple and efficient way, i.e., obtaining still a totally analytic theory? We address all these issues in the present work.

Received: October 15, 2019
Revised: January 10, 2020
Published: January 20, 2020

https://dx.doi.org/10.1021/acs.jpcb.9b09690
J. Phys. Chem. B 2020, 124, 1207−1217

2. THEORY

2.1. Original SPT. A brief recall of SPT is given first to introduce some notations and formulas needed in the following sections. Although its spirit is strictly the same as the original SPT, we present here a pedagogically more appealing formulation based on the chemical potential of the scaled particle[28] instead of the contact radial distribution function, which has been the central quantity considered in the original SPT and many later investigations on SPT. For the chemical potential to insert a hard scaled particle with a radius, R_s (a variable one), into a fluid of hard spheres of radius, R, the following exact but formal result is well known[1]

$$\beta\mu_s(R_s) = \ln\left(\Lambda^3\frac{N\Delta(R_s, R) + 1}{V}\right) - \ln p_0(R_s) \tag{1}$$

where Λ is the thermal wavelength, $\beta = 1/kT$ (k: Boltzmann constant, T: temperature), V is the volume, and N is the number of hard spheres. We consider here the case that the scaled particle has the same mass as the HS particles already in the system and so they have the same thermal wavelength. The scaled particle becomes indistinguishable from the other fluid particles only when $R_s = R$. In eq 1, we account for this indistinguishability by

$$\Delta(R_s, R) = \begin{cases} 1 & R_s = R \\ 0 & R_s \neq R \end{cases} \tag{2}$$

In eq 1, $p_0(R_s)$ is the probability for making a spherical cavity of radius R_s in the HS fluid, and the following exact expression holds

$$p_0(R_s) = 1 + \sum_{n=1}^{\infty} F_n(R_s) \tag{3}$$

with

$$F_n(R_s) = \frac{1}{n!V}\int d\mathbf{r}_s \int d\mathbf{r}_1 \int d\mathbf{r}_2 \ldots \int d\mathbf{r}_n \rho^{(n)}(\mathbf{r}_1, \mathbf{r}_2, \ldots, \mathbf{r}_n) \times \prod_{i=1}^{n} f(|\mathbf{r}_s - \mathbf{r}_i|) \tag{4}$$

where $\rho^{(n)}(\mathbf{r}_1, \mathbf{r}_2, \ldots, \mathbf{r}_n)$ is the distribution function of n particles located, respectively, at $\mathbf{r}_1$, $\mathbf{r}_2$, ..., $\mathbf{r}_n$ and

$$f(|\mathbf{r}_s - \mathbf{r}_i|) = e^{-\beta u_s(|\mathbf{r}_s - \mathbf{r}_i|)} - 1 \tag{5}$$

and

$$u_s(|\mathbf{r}_s - \mathbf{r}_i|) = \begin{cases} \infty & |\mathbf{r}_s - \mathbf{r}_i| < R_s + R \\ 0 & |\mathbf{r}_s - \mathbf{r}_i| \geq R_s + R \end{cases} \tag{6}$$

A property of key importance of eq 3 is that the higher-order terms appear only successively when the radius of the scaled particle increases. For example, we have

$$F_1(R_s) = -\eta\left(1 + \frac{R_s}{R}\right)^3 \quad R_s > -R \tag{7}$$

$$F_2(R_s) = \begin{cases} 0 & -R < R_s < 0 \\ 2\pi\int_{2R}^{2R+2R_s} dr r^2 \rho^{(2)}(r)\Omega_2(r, R_s) & R_s \geq 0 \end{cases} \tag{8}$$

$$F_n(R_s) = 0 \; n \geq 3 \quad -R < R_s \leq R(2 - \sqrt{3})/\sqrt{3} \tag{9}$$

where $\eta = 4\pi\rho R^3/3$ is the packing fraction of hard spheres ($\rho = N/V$ being fluid density) and $\Omega(|\mathbf{r}_1 - \mathbf{r}_2|)$ is the volume of the overlapping region of two spheres having a radius of $R_s + R$ and separated by a distance of $|\mathbf{r}_1 - \mathbf{r}_2|$, which is given by

$$\Omega_2(|\mathbf{r}_1 - \mathbf{r}_2|) = \begin{cases} \frac{2\pi}{3}\left(R_s + R - \frac{|\mathbf{r}_1 - \mathbf{r}_2|}{2}\right)^2\left[2(R_s + R) + \frac{|\mathbf{r}_1 - \mathbf{r}_2|}{2}\right] & 0 < |\mathbf{r}_1 - \mathbf{r}_2| \leq 2(R_s + R) \\ 0 & 2(R_s + R) < |\mathbf{r}_1 - \mathbf{r}_2| \end{cases} \tag{10}$$

Although eqs 1 and 3 indicate a possible road for obtaining chemical potential, one encounters quickly several major obstacles on this road. First, eq 3 is an infinite series and we do not know how it converges for an arbitrary value of R_s. Moreover, only $F_1(R_s)$ has an analytical expression and it is more and more difficult to determine the other higher-order terms.

The strategy used for deriving the original SPT is to use the above exact result in a limited range of R_s, i.e.

$$\beta\mu_s(R_s) = \ln\left(\frac{\Lambda^3}{V}\right) - \ln\left[1 - \eta\left(1 + \frac{R_s}{R}\right)^3\right] \quad -R < R_s \leq 0 \tag{11}$$

For larger values of R_s, the following thermodynamic expression is proposed

$$\beta W(R_s) = \ln\left(\Lambda^3\frac{N\Delta(R_s, R) + 1}{V}\right) + w_0 + w_1 R_s + \frac{1}{2}w_2 R_s^2 + \frac{4\pi R_s^3 \beta P}{3} \quad R_s > 0 \tag{12}$$

where P is the pressure of the HS fluid and the terms of lower powers of R_s account for the surface tension around the scaled particle, which can be considered as a hard spherical wall for the HS fluid. w_2 is related to the surface tension on a planar hard wall and w_1 and w_0 are, respectively, the bending rigidities related to mean and Gauss curvatures. In eq 12, there is no higher-order curvature terms (non-Hadwiger terms), i.e., terms like R_s^{-n} ($n = 1, 2, 3, \ldots$). It is to be pointed out that if eq 12 is replaced by

$$\beta W(R_s) = \ln\left(\Lambda^3\frac{N\Delta(R_s, R) + 1}{V}\right) + \tilde{w}_0 + \tilde{w}_1(R_s + R) + \frac{1}{2}\tilde{w}_2(R_s + R)^2 + \frac{4\pi(R_s + R)^3\beta P}{3} \quad R_s > 0 \tag{13}$$

we obtain the same results for the bulk thermodynamic properties, e.g., pressure and chemical potential, but the results for $\tilde{w}_0$, $\tilde{w}_1$, and $\tilde{w}_2$ are different from those for w_0, w_1, and w_2 in eq 12, since these coefficients are related to surface tension and depend on the choice of the dividing surface.[28] In eq 12, the dividing surface is chosen at the surface of the scaled particle,

https://dx.doi.org/10.1021/acs.jpcb.9b09690
J. Phys. Chem. B 2020, 124, 1207−1217

i.e., at R_s, while in eq 13, it is chosen at the surface of the cavity inside which there is no center of fluid particles, i.e., at $R_s + R$. The latter choice was made in the original SPT and many later investigations on SPT. We prefer the choice at the surface of the scaled particle and will explain later the reason in more detail.

Matching eqs 11 and 12 at $R_s = 0$, i.e., requiring the continuity of the function and the two first derivatives, one obtains

$$w_0 = -\ln(1-\eta) \tag{14}$$

$$w_1 = \frac{3\eta}{1-\eta}\frac{1}{R} \tag{15}$$

$$w_2 = \frac{3\eta}{1-\eta}\left(2 + \frac{3\eta}{1-\eta}\right)\frac{1}{R^2} \tag{16}$$

The chemical potential, μ, and the pressure, P, can be obtained from

$$\beta\mu = \beta W(R_s = R) \tag{17}$$

and Gibbs−Duhem equation, i.e.

$$\frac{\partial(\beta P)}{\partial\rho} = \rho\frac{\partial(\beta\mu)}{\partial\rho} \tag{18}$$

Finally, one obtains

$$\frac{\beta P^{SPT}}{\rho} = \frac{1+\eta+\eta^2}{(1-\eta)^3} \tag{19}$$

$$\beta\mu^{SPT} = \ln(\Lambda^3\rho) - \ln(1-\eta) + \frac{6\eta}{1-\eta} + \frac{9}{2}\left(\frac{\eta}{1-\eta}\right)^2 + \eta\frac{\beta P^{SPT}}{\rho} \tag{20}$$

for the pressure and chemical potential of a bulk HS fluid. Moreover, one obtains also the following dimensionless result for the surface tension of a HS fluid on a spherical hard wall of radius R_s

$$\tilde{\gamma}^{SPT}(R_s) = 4\pi R^2\beta\gamma^{SPT}(R_s) = \tilde{\gamma}_0^{SPT} + \tilde{\gamma}_{-1}^{SPT}\frac{R}{R_s} + \tilde{\gamma}_{-2}^{SPT}\left(\frac{R}{R_s}\right)^2 \tag{21}$$

where $\tilde{\gamma}_0^{SPT}$ is the SPT result for the surface tension of a HS fluid on a planar hard wall

$$\tilde{\gamma}_0^{SPT} = \frac{w_2R^2}{2} = \frac{3\eta}{2(1-\eta)}\left(2 + \frac{3\eta}{1-\eta}\right) \tag{22}$$

and $\tilde{\gamma}_{-1}^{SPT}$ and $\tilde{\gamma}_{-2}^{SPT}$ are, respectively, the bending rigidities related to mean and Gauss curvatures within the framework of SPT

$$\tilde{\gamma}_{-1}^{SPT} = w_1R = \frac{3\eta}{1-\eta} \tag{23}$$

$$\tilde{\gamma}_{-2}^{SPT} = w_0 = -\ln(1-\eta) \tag{24}$$

It is clear from eq 21 that the dividing surface for the hard wall is chosen at R_s.

2.2. Augmented SPT. *2.2.1. Single-Point Matching Formulation.* A conceptually straightforward strategy to include a high-order curvature contribution into an SPT type theory is to add a term proportional to R_s^{-1} into eq 12. However, the immediate difficulty one meets with here is that the divergence of this term at $R_s = 0$ makes impossible the usual matching procedure at this point. This difficulty is directly related to our choice of the dividing surface at R_s. Previously, Corti and co-workers proposed several approaches for improving SPT by including higher-order curvature terms of the form $(R_s + R)^{-n}$ $(n = 1, 2, 3)$, but with the dividing surface chosen at $R_s + R$. As pointed out by Corti et al.,[15−17] the approach by augmenting eq 12 with different higher-order curvature terms can be considered as using a Laurent series for the insertion chemical potential. It is not difficult to admit that the Laurent series written in different ways, i.e., in terms of R_s or $R_s + R$, can have different convergence radii and different convergence rates. Some recent works concerning curved surfaces provided indications that the choice of dividing surfaces really matters. Urrutia reported a systematic investigation on the effect of dividing surfaces on the accuracy of surface tension and bending rigidities given by a large variety of theories with respect to simulations and found that the approximate theories always perform better with the dividing surface chosen at R_s.[43] Moreover, Reindl, Bier, and Dietrich found that more accurate results are obtained from morphological thermodynamics with the choice of dividing surface chosen at R_s rather than at $R_s + R$.[45] These results imply that the Laurent series in terms of R_s converges more rapidly and this is why we chose the dividing surface at R_s rather than at $R_s + R$. We propose below two recipes for removing the singularity at $R_s = 0$. It is also to be noted that the excess adsorption is smaller for the dividing surface at R_s than that with the dividing surface at $R_s + R$ and in consequence, the surface tension is smaller in the former case. Thus, choosing a dividing surface that minimizes surface tension seems to be an advantageous strategy.

One possible way to circumvent the difficulty of divergence at $R_s = 0$ in the matching procedure is to replace $1/R_s$ by $h_n(R_s) = (1 - e^{-R_s/\delta})^n/R_s$, with δ being a real positive constant and n a positive integer. The convergence factor removes the singularity at $R_s = 0$ and keeps the correct asymptotic form of the third-order curvature for large values of R_s. In principle, n can be any positive integer but we can quickly limit the choice of n to a very few cases, which may be interesting for our purpose here. If the original SPT form given in eq 12 is augmented by adding a term proportional to $h_n(R_s)$ with $n \geq 5$, i.e.

$$\beta\Phi(R_s) = \ln\left(\Lambda^3\frac{N\Delta(R_s, R) + 1}{V}\right) + \phi_{-1}h_n(R_s) + \phi_0 + \phi_1R_s + \frac{1}{2}\phi_2R_s^2 + \frac{4\pi R_s^3\beta P}{3} \tag{25}$$

the same results as SPT will be found for ϕ_0, ϕ_1, ϕ_2, and P since the added third-order curvature term does not affect the other terms. However, our objective here is to obtain also improved results for ϕ_0, ϕ_1, ϕ_2, and P by adding the non-Hadwiger term. Hence, we need to consider only the cases of $n = 1, 2, 3, 4$. We worked out all these cases and eliminated the choices of $n = 2, 4$ since the contribution of the non-Hadwiger term is not correctly described with the first non-vanishing Virial coefficient for this term being negative, while the exact

https://dx.doi.org/10.1021/acs.jpcb.9b09690
J. Phys. Chem. B 2020, 124, 1207−1217

one is positive. For the remaining cases, i.e., $n = 1, 3$, the choice of $n = 3$ gives more accurate results for the non-Hadwiger term, and we will present only the results for this case, i.e., substituting $h_3(R_s)$ into eq 25. The determination of the parameter, δ, will be discussed later in Section 3.1.

To determine ϕ_n ($n = -1, 0, 1, 2$), we follow a procedure similar to that used in SPT, i.e., matching eq 25 with eq 1 as follows

$$\beta\mu_s(R_s = 0) = \beta\Phi(R_s = 0) \tag{26}$$

$$\beta\mu_s'(R_s = 0) = \beta\Phi'(R_s = 0) \tag{27}$$

$$\beta\mu_s''(R_s = 0) = \beta\Phi''(R_s = 0) \tag{28}$$

$$\beta\mu_s'''(R_s = 0^+) = \beta\Phi'''(R_s = 0^+) \tag{29}$$

By including the third-order curvature term, we have an additional parameter, ϕ_{-1}, to determine. For this, we resort to an additional condition given in eq 29 for the third derivative of $\mu_s(R_s)$. Since this derivative has a discontinuity at $R_s = 0$, the matching is made at $R_s = 0^+$.

From this matching, we obtain

$$\phi_0 = w_0 = -\ln(1 - \eta) \tag{30}$$

$$\phi_1 = w_1 = \frac{1}{R}\frac{3\eta}{1 - \eta} \tag{31}$$

$$\phi_2 = w_2 - 2\frac{\phi_{-1}}{R}\left(\frac{R}{\delta}\right)^3\frac{1}{R^2} = \frac{1}{R^2}\left[\frac{3\eta}{1 - \eta}\left(2 + \frac{3\eta}{1 - \eta}\right) - 2\frac{\phi_{-1}}{R}\left(\frac{R}{\delta}\right)^3\right] \tag{32}$$

$$\frac{\phi_{-1}}{R} = \left(\frac{\delta}{R}\right)^4\left[\frac{\eta(5 - 2\eta)}{3(1 - \eta)}\frac{\beta P}{\rho} - \frac{5\eta}{3(1 - \eta)} - 6\left(\frac{\eta}{1 - \eta}\right)^2 - 6\left(\frac{\eta}{1 - \eta}\right)^3\right] \tag{33}$$

For the constant term and the coefficient of the linear term, i.e., ϕ_0 and ϕ_1, respectively, we obtain the same results as SPT since the added term, $h_3(R_s)$, does not couple with these terms. From eqs 25 and 30−32, we obtain the following expression for the chemical potential

$$\beta\mu = \beta\Phi(R_s = R) = \ln(\Lambda^3\rho) - \ln(1 - \eta) + \frac{6\eta}{1 - \eta} + \frac{9}{2}\left(\frac{\eta}{1 - \eta}\right)^2 + \eta\frac{\beta P}{\rho} - \frac{\phi_{-1}}{R}\left(\frac{R}{\delta}\right)^3\left[1 - \left(\frac{1 - e^{-R/\delta}}{R/\delta}\right)^3\right] \tag{34}$$

Substituting eq 33 into eq 34 leads to an equation involving chemical potential (μ) and pressure (P). With the help of the Gibbs−Duhem equation, one can eliminate either μ or P and obtain a first-order differential equation for P or μ. Because the obtained differential equation has nonconstant coefficients, it is not possible to solve it analytically. Nevertheless, this difficulty can be circumvented by an iterative procedure to obtain successively analytic results for chemical potential and pressure. One can start the iteration by substituting the SPT result for the pressure (given in eq 19) into the right-hand side (RHS) of eq 33 and obtain

$$\frac{\phi_{-1}}{R} = \left(\frac{\delta}{R}\right)^4\left(\frac{\eta}{1 - \eta}\right)^3\left(2 + \frac{3\eta}{1 - \eta}\right) \tag{35}$$

Substituting eqs 19 and 35 into the RHS of eq 34 yields the following result of the first iteration and we name it ASPT1

$$\beta\mu^{\mathrm{ASPT1}} = \beta\mu^{\mathrm{SPT}} - a(\delta)\left(\frac{\eta}{1 - \eta}\right)^3\left(2 + \frac{3\eta}{1 - \eta}\right) \tag{36}$$

where

$$a(\delta) = \frac{\delta}{R}\left[1 - \left(\frac{1 - e^{-R/\delta}}{R/\delta}\right)^3\right] \tag{37}$$

Using then the result for chemical potential given in eq 36 in the Gibbs−Duhem equation and integrating the latter, we obtain the following ASPT1 result for pressure

$$\frac{\beta P^{\mathrm{ASPT1}}}{\rho} = \frac{\beta P^{\mathrm{SPT}}}{\rho} - 6a(\delta)\left\{\frac{1}{2}\frac{\eta}{1 - \eta}\left[\left(\frac{\eta}{1 - \eta}\right)^3 + \frac{1}{3}\left(\frac{\eta}{1 - \eta}\right)^2 + \frac{1}{3}\frac{\eta}{1 - \eta} - 1\right] - 1 - \frac{1}{\eta}\ln(1 - \eta)\right\} \tag{38}$$

The dimensionless surface tension near a spherical hard wall is given by

$$\tilde{\gamma}^{\mathrm{ASPT1}}(R_s) = 4\pi R^2\beta\gamma^{\mathrm{ASPT1}}(R_s) = \tilde{\gamma}_0^{\mathrm{ASPT1}} + \tilde{\gamma}_{-1}^{\mathrm{ASPT1}}\frac{R}{R_s} + \tilde{\gamma}_{-2}^{\mathrm{ASPT1}}\left(\frac{R}{R_s}\right)^2 + \tilde{\gamma}_{-3}^{\mathrm{ASPT1}}\left(\frac{1 - e^{-R_s/\delta}}{R_s/R}\right)^3 \tag{39}$$

where

$$\tilde{\gamma}_0^{\mathrm{ASPT1}} = \frac{\phi_2 R^2}{2} = \tilde{\gamma}_0^{\mathrm{SPT}} - \tilde{\gamma}_{-3}^{\mathrm{ASPT1}}\left(\frac{R}{\delta}\right)^3 \tag{40}$$

$$\tilde{\gamma}_{-1}^{\mathrm{ASPT1}} = \phi_1 R = \tilde{\gamma}_{-1}^{\mathrm{SPT}} \tag{41}$$

$$\tilde{\gamma}_{-2}^{\mathrm{ASPT1}} = \phi_0 = \tilde{\gamma}_{-2}^{\mathrm{SPT}} \tag{42}$$

$$\tilde{\gamma}_{-3}^{\mathrm{ASPT1}} = \frac{\phi_{-1}}{R} = \left(\frac{\eta}{1 - \eta}\right)^3\left(2 + \frac{3\eta}{1 - \eta}\right)\left(\frac{\delta}{R}\right)^4 \tag{43}$$

In the results given above, there remains a parameter, i.e., δ, to be determined. We will propose, in Section 3.1, a recipe for determining δ and discuss, in more detail, the numerical accuracy of ASPT1. The third-order curvature term introduced into ASPT1 modifies the results for chemical potential, pressure, and planar surface tension, compared to SPT, but gives the same results as SPT for the bending rigidities related to mean and Gauss curvatures, i.e., $\tilde{\gamma}_{-1}^{\mathrm{ASPT1}}$ and $\tilde{\gamma}_{-2}^{\mathrm{ASPT1}}$.

https://dx.doi.org/10.1021/acs.jpcb.9b09690
J. Phys. Chem. B 2020, 124, 1207−1217

2.2.2. Double-Point Matching Formulation. ASPT1 presented above is not an entirely self-contained theory in the sense that it contains one adjustable parameter, i.e., δ. In the following, we will show that it is also possible to develop an augmented scaled particle theory without any adjustable parameter. To circumvent the difficulty due to the divergence of the third-order curvature term, R_s^{-1}, at $R_s = 0$, we propose to extrapolate the exact result for a small-scaled particle, i.e., eq 1, to a thermodynamics expression for a large-scaled particle in two steps instead of the one used for SPT or ASPT1. The first extrapolation is carried out for a scaled particle with a radius in the region of $0 \le R_s \le d = (2/\sqrt{3} - 1)R$ (note that $R + d$ is the radius of a sphere, which can contain at most three hard spheres of radius R). We propose the following expression for the chemical potential of the scaled particle with a radius in this region

$$\beta U(R_s) = \ln\left(\frac{\Lambda^3}{V}\right) + u_0 + u_1 R_s + \frac{1}{2}u_2 {R_s}^2 + \frac{4\pi {R_s}^3 \beta P_1}{3}$$
$$0 \le R_s \le d \tag{44}$$

Since the diverging term, R_s^{-1}, is not included in eq 44, there is no singularity at $R_s = 0$, and we can make the matching of eqs 1 and 44 without any problem, i.e.

$$\beta\mu_s(R_s = 0) = \beta U(R_s = 0) \tag{45}$$
$$\beta\mu_s'(R_s = 0) = \beta U'(R_s = 0) \tag{46}$$
$$\beta\mu_s''(R_s = 0) = \beta U''(R_s = 0) \tag{47}$$
$$\beta\mu_s'''(R_s = 0^+) = \beta U'''(R_s = 0^+) \tag{48}$$

From this matching, we obtain

$$u_0 = w_0 = -\ln(1 - \eta) \tag{49}$$
$$u_1 = w_1 = \frac{3\eta}{1 - \eta}\frac{1}{R} \tag{50}$$
$$u_2 = w_2 = \frac{3\eta}{1 - \eta}\left(2 + \frac{3\eta}{1 - \eta}\right)\frac{1}{R^2} \tag{51}$$
$$8\pi\beta P_1 = \frac{6\eta}{1 - \eta}\left[1 + \frac{9\eta}{1 - \eta} + 9\left(\frac{\eta}{1 - \eta}\right)^2 - \frac{R^3 F_2'''(R_s = 0^+)}{6\eta}\right]\frac{1}{R^3}$$
$$= \frac{6\eta}{1 - \eta}\left[1 + \frac{9\eta}{1 - \eta} + 9\left(\frac{\eta}{1 - \eta}\right)^2 - \frac{3}{2}\left(\frac{\beta P_1}{\rho} - 1\right)\right]\frac{1}{R^3} \tag{52}$$

where

$$F_2'''(R_s = 0^+) = 16\pi^2\rho^2(2R)^3 g(2R^+) = \frac{18\eta}{R^3}\left(\frac{\beta P_1}{\rho} - 1\right) \tag{53}$$

and $g(2R^+)$ is the contact radial distribution function, and the Virial equation for the pressure of a HS fluid was used when going to the last equality in eq 53. It is to be noted that eqs 52 and 53 yield immediately an expression for P_1, which is a first estimation for the pressure, i.e.

$$\frac{\beta P_1}{\rho} = \frac{1}{1 - 2\eta/5}\left[1 + \frac{18}{5}\frac{\eta}{1 - \eta}\left(1 + \frac{\eta}{1 - \eta}\right)\right] \tag{54}$$

At this stage, the above equation of state can be considered as the result of a new variant of scaled particle theory. Since an additional condition, i.e., eq 48, is used, one does not resort to Gibbs−Duhem equation in this first matching. It is to be emphasized that P_1 is not the final result for pressure, and we will use eq 44 and the coefficients given in eqs 49−51 and 54 as the results of a first extrapolation of the chemical potential to insert a larger scaled particle with a radius in the region of $0 \le R_s \le d = (2/\sqrt{3} - 1)R$.

For a scaled particle with a radius larger than d, we use the following expression for its chemical potential including the third-order curvature term

$$\beta W(R_s) = \ln\left(\Lambda^3 \frac{N\Delta(R_s, R) + 1}{V}\right) + w_{-1}\frac{1}{R_s} + w_0 + w_1(R_s - d) + \frac{1}{2}w_2(R_s - d)^2 + \frac{4\pi(R_s - d)^3\beta P}{3},$$
$$R_s \ge d \tag{55}$$

The coefficients in eq 55 (w_n, $n = -1, 0, 1, 2$) are determined by matching eqs 44 and 55 at $R_s = d$, i.e.

$$\beta W(R_s = d) = \beta U(R_s = d) \tag{56}$$
$$\beta W'(R_s = d) = \beta U'(R_s = d) \tag{57}$$
$$\beta W''(R_s = d) = \beta U''(R_s = d) \tag{58}$$
$$\beta W'''(R_s = d) = \beta U'''(R_s = d) \tag{59}$$

We obtain then

$$w_0 = u_0 + Ru_1\frac{d}{R} + \frac{R^2 u_2}{2}\left(\frac{d}{R}\right)^2 + \eta\frac{\beta P_1}{\rho}\left(\frac{d}{R}\right)^3 - \frac{w_{-1}}{R}\frac{R}{d} \tag{60}$$
$$Rw_1 = Ru_1 + R^2 u_2\frac{d}{R} + 3\eta\frac{\beta P_1}{\rho}\left(\frac{d}{R}\right)^2 + \frac{w_{-1}}{R}\left(\frac{R}{d}\right)^2 \tag{61}$$
$$R^2 w_2 = R^2 u_2 + 6\eta\frac{\beta P_1}{\rho}\frac{d}{R} - \frac{2w_{-1}}{R}\left(\frac{R}{d}\right)^3 \tag{62}$$
$$\frac{w_{-1}}{R} = \left(\frac{d}{R}\right)^4 \eta\frac{\beta(P - P_1)}{\rho} \tag{63}$$

Now, we find readily the following result for chemical potential

$$\beta\mu = \beta W(R_s = R) = \ln(\Lambda^3\rho) + \eta\frac{\beta P}{\rho} - \ln(1 - \eta) + \frac{6\eta}{1 - \eta} + \frac{9}{2}\left(\frac{\eta}{1 - \eta}\right)^2 - \left[1 - \left(1 - \frac{d}{R}\right)^4\right]\eta\frac{\beta(P - P_1)}{\rho} \tag{64}$$

Taking derivative with respect to density on both sides of eq 64 and using Gibbs−Duhem equation, i.e., eq 18, allow for obtaining a first-order differential equation either for the chemical potential or for the pressure. Again, the resulting differential equation does not have constant coefficients and this prevents us from solving it analytically. By adopting the same iterative procedure as for ASPT1 (i.e., using the SPT value for pressure on the RHS of eq 64), we obtain the

https://dx.doi.org/10.1021/acs.jpcb.9b09690
J. Phys. Chem. B 2020, 124, 1207−1217

following results (named ASPT2) for chemical potential and pressure after the first iteration

$$\beta\mu^{\mathrm{ASPT2}} = \beta\mu^{\mathrm{SPT}} - A\left[5\frac{\eta}{1-\eta} - \frac{25}{2}\frac{2\eta/5}{1-2\eta/5} - 3\left(\frac{\eta}{1-\eta}\right)^2 + 3\left(\frac{\eta}{1-\eta}\right)^3\right] \tag{65}$$

$$\frac{\beta P^{\mathrm{ASPT2}}}{\rho} = \frac{\beta P^{\mathrm{SPT}}}{\rho} - A\left\{20\left[1 + \frac{1}{\eta}\ln(1-\eta)\right] - \frac{9}{2}\left(\frac{\eta}{1-\eta}\right)^2 + 3\left(\frac{\eta}{1-\eta}\right)^3 - \frac{25}{2}\left[1 + \frac{5}{2\eta}\ln(1-2\eta/5) + \frac{2\eta/5}{1-2\eta/5} - \frac{\eta}{1-\eta}\right]\right\} \tag{66}$$

where

$$A = \frac{256\sqrt{3} - 439}{9} \tag{67}$$

From eq 55, we obtain the following ASPT2 result for the surface tension (dimensionless one) of a HS fluid on a spherical hard wall

$$\tilde{\gamma}^{\mathrm{ASPT2}}(R_s) = 4\pi R^2\beta\gamma^{\mathrm{ASPT2}}(R_s) = \tilde{\gamma}_0^{\mathrm{ASPT2}} + \tilde{\gamma}_{-1}^{\mathrm{ASPT2}}\frac{R}{R_s} + \tilde{\gamma}_{-2}^{\mathrm{ASPT2}}\left(\frac{R}{R_s}\right)^2 + \tilde{\gamma}_{-3}^{\mathrm{ASPT2}}\left(\frac{R}{R_s}\right)^3 \tag{68}$$

where

$$\tilde{\gamma}_0^{\mathrm{ASPT2}} = \tilde{\gamma}_0^{\mathrm{SPT}} - 4\tilde{\gamma}_{-3}^{\mathrm{ASPT2}}\left(\frac{3}{2\sqrt{3}-3}\right)^3 \tag{69}$$

$$\tilde{\gamma}_{-1}^{\mathrm{ASPT2}} = \tilde{\gamma}_{-1}^{\mathrm{SPT}} + 6\tilde{\gamma}_{-3}^{\mathrm{ASPT2}}\left(\frac{3}{2\sqrt{3}-3}\right)^2 \tag{70}$$

$$\tilde{\gamma}_{-2}^{\mathrm{ASPT2}} = \tilde{\gamma}_{-2}^{\mathrm{SPT}} - 4\tilde{\gamma}_{-3}^{\mathrm{ASPT2}}\frac{3}{2\sqrt{3}-3} \tag{71}$$

$$\tilde{\gamma}_{-3}^{\mathrm{ASPT2}} = \left\{\frac{\eta}{1-\eta}\left[5 - \frac{3\eta}{1-\eta} + 3\left(\frac{\eta}{1-\eta}\right)^2\right] - \frac{25}{2}\frac{2\eta/5}{1-2\eta/5}\right\}\left(\frac{2\sqrt{3}-3}{3}\right)^4 \tag{72}$$

It is to be pointed out that the double matching procedure used above for obtaining ASPT2 is in the same spirit as the method of multiple interpolation functions proposed by Corti and co-workers. Nevertheless, we choose, as for ASPT1, the dividing surface for defining the cavity at R_s rather than at $R_s + R$ in the previous work of Corti and co-workers.[17,18]

By considering the exact results of low order cluster integrals, Urrutia proposed some empirical expressions for the surface tension of a HS fluid on a planar hard wall, as well as the two first bending rigidities on a spherical hard wall.[43] The analytic results given explicitly in ref 43 are for a dividing surface chosen at $R_s + R$. For the comparison with our results to be discussed in the next section, we transform them to those for a dividing surface chosen at R_s, i.e.

$$\tilde{\gamma}_0^{\mathrm{Urrutia}} = \tilde{\gamma}_0^{\mathrm{SPT}} - \left[\frac{81}{70} + \frac{237}{76}\eta - \frac{27}{2}\eta^2(1-\eta)\right]\left(\frac{\eta}{1-\eta}\right)^3 \tag{73}$$

$$\tilde{\gamma}_{-1}^{\mathrm{Urrutia}} = \tilde{\gamma}_{-1}^{\mathrm{SPT}} + \left(\frac{\eta}{1-\eta}\right)^2\left[\left(9 + \frac{81\sqrt{3}}{16\pi}\right)\eta(1+1.2\eta) - \frac{396+123\eta}{35}\frac{\eta}{1-\eta} + 27\eta^3\right] \tag{74}$$

$$\tilde{\gamma}_{-2}^{\mathrm{Urrutia}} = \frac{\eta}{1-\eta} + \left[-\frac{1}{2} + \left(\frac{185}{42} + \frac{81\sqrt{3}}{16\pi}\right)\eta + 1.2\left(9 + \frac{81\sqrt{3}}{16\pi}\right)\eta^2 + \frac{27}{2}\eta^3\right]\left(\frac{\eta}{1-\eta}\right)^2 - \left(\frac{501}{70} + \frac{85}{76}\eta\right)\left(\frac{\eta}{1-\eta}\right)^3 - 2.16\pi(1+3\eta)\eta^4 \tag{75}$$

In such a transformation, the expression for pressure is needed and we used Carnahan−Starling equation as did Urrutia.

3. RESULTS AND DISCUSSION

3.1. Determination of the Adjustable Parameter in ASPT1. Before ASPT1 can be used to obtain numerical results, the parameter, δ, has to be determined first. An appealing recipe for this is to adjust it in such a way that the pressure given by eq 38 is as close as that of the Carnahan−Starling equation, which has the following expression

$$\frac{\beta P^{\mathrm{CS}}}{\rho} = \frac{\beta P^{\mathrm{SPT}}}{\rho} - \left(\frac{\eta}{1-\eta}\right)^3 \tag{76}$$

Since P^{SPT} is different from P^{CS} only at high fluid densities, requiring $P^{\mathrm{ASPT1}} = P^{\mathrm{CS}}$ at a high fluid density (with $\eta = 0.5$ being chosen here) should allow for obtaining accurate values of pressure from ASPT1. This leads to the following equation for determining δ

$$\frac{\delta}{R}\left[1 - \left(\frac{1-\mathrm{e}^{-R/\delta}}{R/\delta}\right)^3\right] = \frac{1}{4(3\ln 2 - 1)} \tag{77}$$

From eqs 37 and 38, we see that any positive root of eq 77 can decrease the pressure given by SPT so that P^{ASPT1} becomes closer to P^{CS}, thus improving the results of SPT. Solving eq 77, we find only one positive root, i.e., $\delta/R = 0.234499$. With this parameter being adjusted at a single density point, the curve given by ASPT1 (see Figure 1) overlaps that of the Carnahan−Starling equation perfectly over the whole density region. This indicates that our assumption that δ is independent of density is a quite plausible one. Alternatively, if we require $P^{\mathrm{ASPT1}} = P^{\mathrm{ASPT2}}$ at $\eta = 0.5$, we obtain the following equation for δ

https://dx.doi.org/10.1021/acs.jpcb.9b09690
J. Phys. Chem. B 2020, 124, 1207−1217

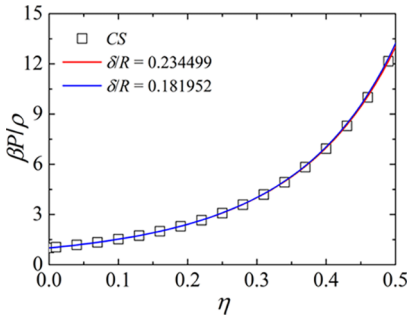

Figure 1. Pressure of a hard sphere fluid given by ASPT1 compared to the result given by the Carnahan−Starling equation[46] (open squares): (1) red line for the adjustable parameter, $\delta/R = 0.234499$ (see Section 3.1); (2) blue line for the adjustable parameter $\delta/R = 0.181952$ (see Section 3.1).

$$\frac{\delta}{R}\left[1 - \left(\frac{1 - e^{-R/\delta}}{R/\delta}\right)^3\right] = \frac{256\sqrt{3} - 439}{216(3\ln 2 - 1)}\left(\frac{123}{8} + \frac{125}{2}\ln 5 - 165\ln 2\right) \tag{78}$$

From this equation, we find $\delta/R = 0.181952$. The two values for δ give quite close results for pressure (see Figure 1), and in the following discussions, we will use $\delta/R = 0.234499$ for ASPT1.

3.2. Virial Coefficients for Pressure and Surface Tension. For a HS fluid, the exact and analytical results for the first four Virial coefficients of pressure are known, and Monte Carlo simulation results are available for higher-order Virial coefficients up to the tenth.[47] Comparison of the Virial coefficients given by an approximate theory to the exact ones provides an appraisal for the accuracy of the approximate theory. The Virial expansion of pressure describes the deviation from the equation of state for an ideal gas at low densities, i.e.

$$\frac{\beta P}{\rho} = 1 + \sum_{i=2}^{\infty} B_i \eta^{i-1} \tag{79}$$

where B_i is the ith Virial coefficient. It is well known that SPT gives the exact results for the second and third Virial coefficients but approximately for higher ones. From eqs 38 and 66, one can show straightforwardly that both ASPT1 and ASPT2 give the exact second and third Virial coefficients as SPT but correct the SPT results for higher-order coefficients. The Virial coefficients, up to the tenth, given by ASPT1 and ASPT2 are presented in Table 1 along with the exact results and those given by SPT and the Carnahan−Starling equation (CS). Some previous efforts have been made to develop SPT type approaches by using the Carnahan−Starling equation as input, e.g., CS−SPT$_M$ by Siderius and Corti[17] and modified fundamental measure theory (MFMT) by Hansen-Goos and Roth.[48] By construction, such approaches give the same Virial coefficients for pressure as the Carnahan−Starling equation. So, we will not show them in Table 1 in addition to those given by the CS equation.

The standard deviation provides a measure for the overall accuracy, i.e.

Table 1. Virial Coefficients for the Pressure of a Hard Sphere Fluid

n	exact[47]	SPT	CS	ASPT1	ASPT2
2	4	4	4	4	4
3	10	10	10	10	10
4	18.3647	19	18	18.6526	18.5595
5	28.2245(10)	31	28	29.3325	29.1675
6	39.81545(15)	46	40	41.368	41.5656
7	53.3418(15)	64	54	54.0742	55.631
8	68.534(88)	85	70	66.7614	71.3043
9	85.805(58)	109	88	78.7375	88.5556
10	105.8(4)	136	108	89.3093	107.369

$$\Delta = \sqrt{\sum_{i=2}^{10} (B_i - B_i^{\text{exact}})^2} \Big/ \sum_{i=2}^{10} B_i^{\text{exact}} \tag{80}$$

From the results in Table 1, we find that $\Delta^{SPT} = 10.48\%$, $\Delta^{ASPT1} = 4.393\%$, $\Delta^{ASPT2} = 1.254\%$, and $\Delta^{CS} = 0.8528\%$. ASPT1 reduces by half the standard deviation compared to SPT. The results in Table 1 show clearly that the accuracy of ASPT1 deteriorates for high-order Virial coefficients (from B_8). The overall accuracy of ASPT2 is excellent and very close to that of the Carnahan−Starling equation.

The Virial coefficients for $\tilde{\gamma}_0$ given by ASPT1 and ASPT2 are presented in Table 2 along with the exact results and those from some other theories. ASPT1 and ASPT2 give both the exact second and third Virial coefficients for this quantity, and their respective errors for the fourth Virial coefficient are 6.346% and 3.823%, while SPT and MFMT[48] have, respectively, an error of 10.67% and −4.703% for this quantity. It is to be noted that CS−SPT$_M$ of Siderius and Corti[17] gives an excellent result for the fourth Virial coefficient of $\tilde{\gamma}_0$ with an error of 0.0996% only. By construction, the empirical formulas for surface tension proposed by Urrutia, i.e., eqs 73−75 give the exact Virial coefficients up to the fourth order, which are not reproduced either in Table 2 or in Tables 3 and 4.

Table 2. Virial Coefficients for the Surface Tension of a HS Fluid on a Plane Hard Wall $\tilde{\gamma}_0$

n	exact[43,44]	SPT	MFMT[48]	CS−SPT$_M$[17]	ASPT1	ASPT2
2	3	3	3	3	3	3
3	7.5	7.5	7.5	7.5	7.5	7.5
4	10.8429	12	10.333	10.8537	11.531	11.2574

Table 3. Virial Coefficients for Mean-Curvature Bending Rigidity, $\tilde{\gamma}_{-1}$

n	exact[43,44]	SPT	MFMT[48]	CS−SPT$_M$[17]	ASPT1	ASPT2
2	3	3	3	3	3	3
3	3	3	3	3	3	3
4	3.47682	3	3.333	0.90253	3	3.17231

Table 4. Virial Coefficients for Gauss-Curvature Bending Rigidity, $\tilde{\gamma}_{-2}$

n	exact[43,44]	SPT	MFMT[48]	CS−SPT$_M$[17]	ASPT1	ASPT2
2	1	1	1	1	1	1
3	0.5	0.5	0.5	0.5	0.5	0.5
4	0.03872	0.3333	0.3333	6.76477	0.3333	0.31556

https://dx.doi.org/10.1021/acs.jpcb.9b09690
J. Phys. Chem. B 2020, 124, 1207−1217

Table 5. Virial Coefficients for Third-Order-Curvature Bending Rigidity, $\tilde{\gamma}_{-3}$

n	exact[43,44]	EFMT[44]	CS−SPT$_M$[17]	ASPT1	ASPT2
2	0	0	0	0	0
3	0	0	0	0	0
4	2.481×10^{-1}	9.842×10^{-2}	−9.042	6.048×10^{-3}	6.873×10^{-4}

The Virial coefficients for $\tilde{\gamma}_{-1}$ given by ASPT1 and ASPT2 are presented in Table 3 along with the exact results and those from some other theories. ASPT1 and ASPT2 give both the exact second and third Virial coefficients for this quantity and their respective errors for the fourth Virial coefficient are −13.71% and −8.758%, while SPT and MFMT have, respectively, an error of −13.71% and −4.137% for this quantity. It is quite striking that CS−SPT$_M$ largely underestimates the fourth Virial coefficient of $\tilde{\gamma}_{-1}$ and gives a result even worse than the original SPT.

The Virial coefficients for $\tilde{\gamma}_{-2}$ given by ASPT1 and ASPT2 are presented in Table 4 along with the exact results and those from some other theories. Although all of the theories give the exact second and third Virial coefficients for this quantity, they all overestimate this quantity by about 1 order of magnitude except CS−SPT$_M$, which overestimates the fourth Virial coefficient of $\tilde{\gamma}_{-2}$ by more than 2 orders of magnitude. Our ASPT2 gives a slightly better result than the other theories.

The Virial coefficients for the third-order bending rigidity are presented in Table 5. The exact calculations show that the second and the third Virial coefficients for this quantity vanish identically. Both ASPT1 and ASPT2 as well as CS−SPT$_M$ and the extended fundamental measure theory (EFMT) proposed by Hansen-Goos give exactly the same starting density dependence, i.e., like ρ^3. ASPT1 and ASPT2 underestimate largely the amplitude of the fourth Virial coefficient although the sign is correct. EFMT gives a better but also underestimated value for this quantity. However, CS−SPT$_M$ gives a qualitatively incorrect result for the fourth Virial coefficient of $\tilde{\gamma}_{-3}$ with a wrong sign.

Before closing this subsection, it is useful to make a point relating to the question of whether including some high-order curvature terms necessarily improves SPT. From the above discussions, the answer to this question is clearly negative. CS−SPT$_M$ takes into account several high-order curvature terms (more than in our ASPT1 or ASPT2). By construction, CS−SPT$_M$ gives the same results for the bulk thermodynamic properties as the Carnahan−Starling equation. Moreover, its result for the surface tension at a planar wall is excellent. However, its results for the bending rigidities related to mean and Gauss curvatures are even worse than the original SPT. The prediction of CS−SPT$_M$ for the fourth Virial coefficient of $\tilde{\gamma}_{-3}$ has even a wrong sign. Now, it is clear that including higher-order curvature terms does not guarantee to obtain a well-balanced new approach that gives an overall improvement with respect to the original SPT.

3.3. Bulk and Surface Thermodynamic Properties at High Densities. In this subsection, we will present the results of ASPT1 and ASPT2 and appraise their accuracy over the whole region of fluid density. Figure 2 shows that for the pressure, both ASPT1 and ASPT2 give results in excellent agreement with those of Monte Carlo simulation.

It is to be emphasized that our ASPT1 and ASPT2 improve not only the bulk thermodynamic properties of a hard sphere fluid but also its surface tension. For the surface tension of a hard sphere fluid on a plane hard wall, ASPT1 and ASPT2

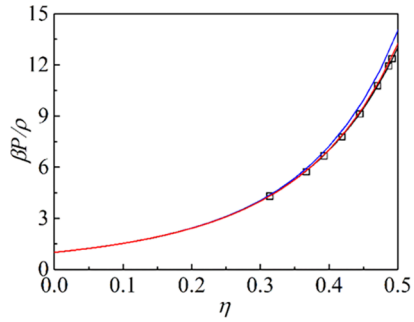

Figure 2. Pressure of a hard sphere fluid. ASPT1: black line; ASPT2: red line; Monte Carlo simulation:[15] black square; SPT: blue line.

improve significantly the results of SPT, in particular in the high-density region (see Figure 3). The empirical formula

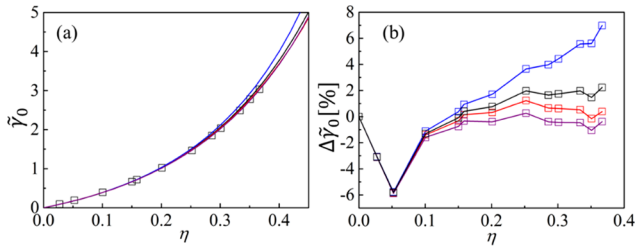

Figure 3. (a) Surface tension of a hard sphere fluid on a plane hard wall. Molecular dynamics simulation:[42] black squares; Urrutia's formula:[43] purple line; ASPT1: black line; ASPT2: red line; SPT: blue line. (b) Corresponding relative errors of different theories with respect to MD results.

proposed by Urrutia, i.e., eq 73, is currently the most accurate one for the surface tension of a HS fluid on a planar hard wall and our ASPT2 has the same accuracy as it (see Figure 3b). From Figure 3b, we see Urrutia's formula, and our ASPT1 and ASPT2 give results accurate to 2%. We believe that the unusual errors at low fluid densities ($\eta < 0.1$) are due to the numerical errors of the simulation results for small quantities.

As we pointed out in Section 2.2.1, ASPT1, by construction, gives the same results for the two bending rigidities, i.e., γ_{-1} and γ_{-2}, as SPT. In Figure 4, the results of ASPT2 for γ_{-1} are compared to the simulation ones, Urrutia's empirical formula, eq 74, and those of SPT. ASPT2 underestimates slightly γ_{-1} at high densities but still gives quite accurate results compared to molecular dynamics simulation and improves SPT results. Urrutia's formula gives accurate results up to $\eta = 0.4$ but shows an inflection at a higher density and passes even below the SPT curve (see Figure 4a).

ASPT2 overestimates γ_{-2}, in particular, in the region of high density (see Figure 5) but still slightly improves SPT results. Urrutia's empirical formula for this quantity, eq 75, gives very accurate results. Finally, the results for the third-order-curvature bending rigidity are presented in Figure 6. The simulation results of Laird et al.[41] show a quite complicated variation of this term with the fluid density: positive at low

https://dx.doi.org/10.1021/acs.jpcb.9b09690
J. Phys. Chem. B 2020, 124, 1207−1217

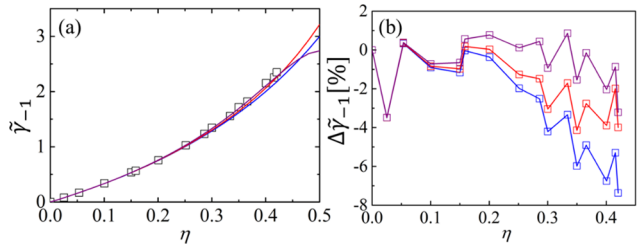

Figure 4. (a) Bending rigidity related to mean curvature, γ_{-1}, of a hard sphere fluid on a spherical hard wall. Molecular dynamics simulation:[41] black squares; Urrutia's formula:[43] purple line; ASPT2: red line; SPT: blue line (ASPT1 gives the same results as SPT). (b) Corresponding relative errors of different theories with respect to MD results.

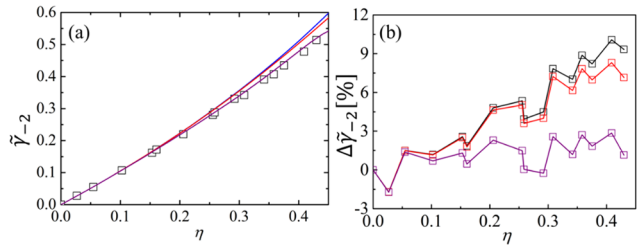

Figure 5. (a) Bending rigidity related to Gauss curvature, γ_{-2}, of a hard sphere fluid on a spherical hard wall. Molecular dynamics simulation:[41] black squares; Urrutia's formula:[43] purple line; ASPT2: red line; SPT: blue line (ASPT1 gives the same results as SPT). (b) Corresponding relative errors of different theories with respect to MD results.

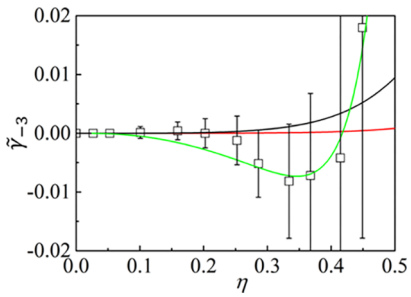

Figure 6. Third-order-curvature bending rigidity, $\tilde{\gamma}_{-3}$, for a HS fluid on a spherical hard wall. Molecular dynamics simulation:[41] black squares; EFMT:[44] green line; ASPT1: black line; ASPT2: red line.

densities, negative in the intermediate region of density, and again positive at high densities. Our ASPT1 and ASPT2 both give a monotonous increase of this quantity with the fluid density and ASPT2 gives a much smaller contribution of this bending rigidity than ASPT1. We have seen that the fourth Virial coefficient given by ASPT2 is smaller than that of ASPT1 by 1 order of magnitude. The EFMT proposed by Hansen-Goos describes this complicated variation very well (see Figure 6). The two additional scaled-particle variables used by Hansen-Goos make it impossible to solve analytically the EFMT equation. It is to be noted that the definition of such variables is not unique. We tried some possible choices but they do not allow for solving analytically the extended FMT either. The analytical expression for the third-order-curvature bending rigidity, proposed by Hansen-Goos, is an ad hoc one obtained by using Urrutia's empirical formula for surface tension of a HS fluid on a planar hard wall as input. So, EFMT is not a self-containing theory. Because of its small amplitude, the determination of γ_{-3} by simulation is extremely difficult and tainted with large computational errors (see Figure 6). It is to be noted that the locus of the upper ends of the error bars for the simulation data never goes to the negative side. Moreover, all of the other terms of the surface tension for a HS fluid on a hard spherical wall are positive and monotonously increasing with fluid density. We believe that more accurate simulation data for the third-order-curvature bending rigidity are needed. This issue deserves also further theoretical investigations, in line with the call made by Hansen-Goos,[44] for further theoretical studies to determine the points at which γ_{-3} changes its sign.

4. CONCLUSIONS

Two approaches are proposed for augmenting the expression of the cavity-forming work in SPT by only one non-Hadwiger term, i.e., the third-order curvature. This strategy is simpler than the previous similar approaches. Since only one additional term is introduced, four exact conditions are enough to match the augmented expression of the cavity-forming work for a large cavity to the exact results of this work for small cavities. We believe that the success of our simple strategy is due to the choice of the dividing surface for defining the cavity at the surface of the scaled particle instead of the surface of the excluding sphere of the centers of the hard spheres around the scaled particle. The difficulty with this choice of dividing surface is that it prevents a straightforward matching procedure because of a divergence problem. We proposed two methods to circumvent this difficulty, one for a single matching formulation and the other for a double matching procedure. The thus obtained new approaches named ASPT1 and ASPT2 are totally analytical. Both of them give excellent results for bulk thermodynamic properties of a HS fluid, with the accuracy equivalent to that of the Carnahan−Starling equation. Moreover, both ASPT1 and ASPT2 give very accurate results for the surface tension of a HS fluid on a plane hard wall over the whole fluid density region, in particular, ASPT2 has the same accuracy as the empirical formula proposed by Urrutia, which is currently the most accurate one for this quantity. By construction, ASPT1 does not improve the contributions from the mean and Gauss curvatures with respect to SPT. It is really remarkable that ASPT2 improves all of the curvature terms to the surface tension, compared to SPT. Its simplicity and good accuracy for both bulk and surface thermodynamic properties make ASPT2 a very attractive theory for studying complex inhomogeneous fluids, e.g., those confined in complex porous media. ASPT2 gives a monotonously increasing third-order-curvature bending rigidity as a function of fluid density while simulation results show apparently a more complicated variation of this quantity with the fluid density. Further simulations with better numerical accuracy and theoretical investigations on the sign of this quantity are needed.

AUTHOR INFORMATION

Corresponding Authors

S. L. Zhao − *State Key Laboratory of Chemical Engineering and School of Chemical Engineering, East China University of Science and Technology, 200237 Shanghai, China;* orcid.org/0000-0002-9547-4860; Email: szhao@ecust.edu.cn

W. Dong − *Université de Lyon, CNRS, Ecole Normale Supérieure de Lyon, Université Lyon 1, Laboratoire de Chimie,*

https://dx.doi.org/10.1021/acs.jpcb.9b09690
J. Phys. Chem. B 2020, 124, 1207−1217

UMR 5182, 69364 Lyon, France; orcid.org/0000-0003-3773-1029; Email: wei.dong@ens-lyon.fr

Authors

C. Z. Qiao − *State Key Laboratory of Chemical Engineering and School of Chemical Engineering, East China University of Science and Technology, 200237 Shanghai, China; Université de Lyon, CNRS, Ecole Normale Supérieure de Lyon, Université Lyon 1, Laboratoire de Chimie, UMR 5182, 69364 Lyon, France*

H. L. Liu − *School of Chemistry and Molecular Engineering, East China University of Science and Technology, 200237 Shanghai, China;* orcid.org/0000-0002-5682-2295

Complete contact information is available at: https://pubs.acs.org/10.1021/acs.jpcb.9b09690

Notes

The authors declare no competing financial interest.

■ ACKNOWLEDGMENTS

This work is supported by National Natural Science Foundation of China (Nos. 21878078 and U1707602) and the 111 Project of China (No. B08021). C.Z.Q. is grateful to Campus France for an Eiffel scholarship, to la Région Rhône-Alpes (France) for a CMIRA scholarship, and to the Chinese Scholarship Council for the visiting fellowship.

■ REFERENCES

(1) Reiss, H.; Frisch, H. L.; Lebowitz, J. L. Statistical Mechanics of Rigid Spheres. *J. Chem. Phys.* **1959**, *31*, 369−380.
(2) Stillinger, F. H. Structure in Aqueous Solutions of Nonpolar Solutes from the Standpoint of Scaled-Particle Theory. *J. Solution Chem.* **1973**, *2*, 141.
(3) Ashbaugh, H. S.; Pratt, L. R. Colloquium: Scaled Particle Theory and the Length Scales of Hydrophobicity. *Rev. Mod. Phys.* **2006**, *78*, 159−178.
(4) Reiss, H.; Frisch, H. L.; Helfand, E.; Lebowitz, J. L. Aspects of the Statistical Thermodynamics of Real Fluids. *J. Chem. Phys.* **1960**, *32*, 119−124.
(5) Reiss, H. Scaled Particle Methods in the Statisitical Thermodynamicsof Fluids. *Adv. Chem. Phys.* **1965**, *9*, 1−84.
(6) Helfand, E.; Frisch, H. L.; Lebowitz, J. L. Theory of the Two- and One-Dimensional Rigid Sphere Fluids. *J. Chem. Phys.* **1961**, *34*, 1037−1042.
(7) Lebowitz, J. L.; Helfand, E.; Praestgaard, E. Scaled Particle Theory of Fluid Mixtures. *J. Chem. Phys.* **1965**, *43*, 774−779.
(8) Tully-Smith, D. M.; Reiss, H. Further Development of Scaled Particle Theory of Rigid Sphere Fluids. *J. Chem. Phys.* **1970**, *53*, 4015−4025.
(9) Mandell, M. J.; Reiss, H. Scaled Particle Theory: Solution to the Complete Set of Scaled Particle Theory Conditions: Applications to Surface Structure and Dilute Mixtures. *J. Stat. Phys.* **1975**, *13*, 113−128.
(10) Bergmann, E. Scaled Particle Theory for Non-Additive Hard Spheres General Theory and Solution of the Widom-Rowlinson Model. *Mol. Phys.* **1976**, *32*, 237−256.
(11) Tenne, R.; Bergmann, E. Scaled Particle Theory for Nonadditive Hard Spheres: Solutions for General Positive Non-additivity. *Phys. Rev. A* **1978**, *17*, 2036−2045.
(12) Cotter, M. A.; Stillinger, F. H. Extension of Scaled Particle Theory for Rigid Disks. *J. Chem. Phys.* **1972**, *57*, 3356.
(13) Stillinger, F. H.; Debenedetti, P. G.; Chatterjee, S. Scaled Particle Theory for Hard Sphere Pairs. I. Mathematical Structure. *J. Chem. Phys.* **2006**, *125*, No. 204504.
(14) Chatterjee, S.; Debenedetti, P. G.; Stillinger, F. H. Scaled Particle Theory for Hard Sphere Pairs. II. Numerical Analysis. *J. Chem. Phys.* **2006**, *125*, No. 204505.
(15) Heying, M.; Corti, D. S. Scaled Particle Theory Revisited: New Conditions and Improved Predictions of the Properties of the Hard Sphere Fluid. *J. Phys. Chem. B* **2004**, *108*, 19756−19768.
(16) Siderius, D. W.; Corti, D. S. Thermodynamically Consistent Adaptation of Scaled Particle Theory to an Arbitrary Hard-Sphere Equation of State. *Ind. Eng. Chem. Res.* **2006**, *45*, 5489−5500.
(17) Siderius, D. W.; Corti, D. S. On the Use of Multiple Interpolation Functions in Scaled Particle Theory to Improve the Predictions of the Properties of the Hard-Sphere Fluid. *J. Chem. Phys.* **2007**, *127*, No. 144502.
(18) Heying, M.; Corti, D. S. On the Use of Multiple Interpolation Series in Scaled Particle Theory: Improved Predictions and Limitations. *Mol. Phys.* **2014**, *112*, 2160−2175.
(19) Siderius, D. W.; Corti, D. S. Extension of Scaled Particle Theory to Inhomogeneous Hard Particle Fluids. I. Cavity Growth at a Hard Wall. *Phys. Rev. E* **2005**, *71*, No. 036141.
(20) Siderius, D. W.; Corti, D. S. Extension of Scaled Particle Theory to Inhomogeneous Hard Particle Fluids. II. Theory and Simulation of Fluid Structure Surrounding a Cavity That Intersects a Hard Wall. *Phys. Rev. E* **2005**, *71*, No. 036142.
(21) Siderius, D. W.; Corti, D. S. Extension of Scaled Particle Theory to Inhomogeneous Hard Particle Fluids. III. Entropy Force Exerted on a Cavity That Intersects a Hard Wall. *Phys. Rev. E* **2007**, *75*, No. 011108.
(22) Holovko, M.; Dong, W. A Highly Accurate and Analytic Equation of State for a Hard Sphere Fluid in Random Porous Media. *J. Phys. Chem. B* **2009**, *113*, 6360−6365.
(23) Holovko, M. F.; Shmotolokha, V. I.; Dong, W. Analytical Theory of One- and Two-Dimensional Hard Sphere Fluids in Random Porous Media. *Condens. Matter Phys.* **2010**, *13*, No. 23607.
(24) Patsahan, T.; Holovko, M.; Dong, W. Fluids in Porous Media. III. Scaled Particle Theory. *J. Chem. Phys.* **2011**, *134*, No. 074503.
(25) Holovko, M.; Patsahan, T.; Dong, W. One-Dimensional Hard Rod Fluid in a Disordered Porous Medium: Scaled Particle Theory. *Condens. Matter Phys.* **2012**, *15*, No. 23607.
(26) Holovko, M.; Patsahan, T.; Dong, W. Fluids in Random Porous Media: Scaled Particle Theory. *Pure Appl. Chem.* **2012**, *85*, 115−133.
(27) Chen, W.; Zhao, S. L.; Holovko, M.; Chen, X. S.; Dong, W. Scaled Particle Theory for Multicomponent Hard Sphere Fluids Confined in Random Porous Media. *J. Phys. Chem. B* **2016**, *120*, 5491−5504.
(28) Dong, W.; Chen, X. S. Scaled Particle Theory for Bulk and Confined Fluids: A Review. *Sci. China: Phys., Mech. Astron.* **2018**, *61*, No. 070501.
(29) Tolman, R. C. The Effect of Droplet Size on Surface Tension. *J. Chem. Phys.* **1949**, *17*, 333.
(30) Mecke, K. R.; Buchert, T.; Wagner, H. Robust Morphological Measures for Large-Scale Structure. *Astron. Astrophys.* **1994**, *288*, 697−704.
(31) Mecke, K. R. Morphological Thermodynamics of Composite Media. *Fluid Phase Equilib.* **1998**, *150*−*151*, 591−598.
(32) Mecke, K. R. Exact Moments of Curvature Measures in the Boolean Model. *J. Stat. Phys.* **2001**, *102*, 1343−1381.
(33) Arns, C. H.; Knackstedt, M. A.; Pinczewski, W. V.; Mecke, K. R. Euler-Poincaré Characteristics of Classes of Disordered Media. *Phys. Rev. E* **2001**, *63*, No. 031112.
(34) Arns, C. H.; Knackstedt, M. A.; Mecke, K. R. Reconstructing Complex Materials via Effective Grain Shapes. *Phys. Rev. Lett.* **2003**, *91*, No. 215506.
(35) König, P.-M.; Roth, R.; Mecke, K. R. Morphological Thermodynamics of Fluids: Shape Dependence of Free Energies. *Phys. Rev. Lett.* **2004**, *93*, No. 160601.
(36) Roth, R.; Harano, Y.; Kinoshita, M. Morphometric Approach to the Solvation Free Energy of Complex Molecules. *Phys. Rev. Lett.* **2006**, *97*, No. 078101.

(37) Hansen-Goos, H.; Roth, R.; Mecke, K.; Dietrich, S. Solvation of Proteins: Linking Thermodynamics to Geometry. *Phys. Rev. Lett.* **2007**, *99*, No. 128101.
(38) Jin, Z.; Kim, J.; Wu, J. Shape Effect on Nanoparticle Solvation: A Comparison of Morphometric Thermodynamics and Microscopic Theories. *Langmuir* **2012**, *28*, 6997−7006.
(39) Klain, D. A. A Short Proof of Hadwiger's Characterization Theorem. *Mathematika* **1995**, *42*, 329.
(40) Chen, B. A Simplified Elementary Proof of Hadwiger's Volume Theorem. *Geom. Dedicata* **2004**, *105*, 107−120.
(41) Laird, B. B.; Hunter, A.; Davidchack, R. L. Interfacial Free Energy of a Hard-Sphere Fluid in Contact with Curved Hard Surfaces. *Phys. Rev. E* **2012**, *86*, No. 060602.
(42) Blokhuis, E. M. Existence of a Bending Rigidity for a Hard-Sphere Liquid near a Curved Hard Wall: Validity of the Hadwiger Theorem. *Phys. Rev. E* **2013**, *87*, No. 022401.
(43) Urrutia, I. Bending Rigidity and Higher-Order Curvature Terms for the Hard-Sphere Fluid near a Curved Wall. *Phys. Rev. E* **2014**, *89*, No. 032122.
(44) Hansen-Goos, H. Communication: Non-Hadwiger Terms in Morphological Thermodynamics of Fluids. *J. Chem. Phys.* **2014**, *141*, No. 171101.
(45) Reindl, A.; Bier, M.; Dietrich, S. Implications of Interface Conventions for Morphometric Thermodynamics. *Phys. Rev. E* **2015**, *91*, No. 022406.
(46) Carnahan, N. F.; Starling, K. E. Equation of State for Nonattracting Rigid Spheres. *J. Chem. Phys.* **1969**, *51*, 635−636.
(47) *Theory and Simulation of Hard-Sphere Fluids and Related Systems*; Mulero, A., Ed.; Lecture Notes in Physics; Springer: Berlin, 2008; Vol. 753.
(48) Hansen-Goos, H.; Roth, R. Density Functional Theory for Hard-Sphere Mixtures: The White Bear Version Mark II. *J. Phys.: Condens. Matter* **2006**, *18*, 8413−8425.

https://dx.doi.org/10.1021/acs.jpcb.9b09690
J. Phys. Chem. B 2020, 124, 1207−1217